We are IntechOpen, the world's leading publisher of Open Access books Built by scientists, for scientists

4,800
Open access books available

122,000
International authors and editors

135M
Downloads

Our authors are among the

154
Countries delivered to

TOP 1%
most cited scientists

12.2%
Contributors from top 500 universities

CLARIVATE ANALYTICS BOOK CITATION INDEX INDEXED

WEB OF SCIENCE™

Selection of our books indexed in the Book Citation Index in Web of Science™ Core Collection (BKCI)

Interested in publishing with us?
Contact book.department@intechopen.com

Numbers displayed above are based on latest data collected.
For more information visit www.intechopen.com

6

Nonparametric Statistical Downscaling of Precipitation from Global Climate Models

Paul Nyeko-Ogiramoi[1,2,3], Patrick Willems[2],
Gaddi Ngirane-Katashaya[3] and Victor Ntegeka[2]
[1]*Ministry of Water and Environment, Directorate of Water Development, Rural Water and Sanitation Department, Kampala,*
[2]*Katholieke Universiteit Leuven, Civil Engineering Department, Hydraulics Laboratory, Leuven,*
[3]*Makerere University, Civil Engineering Department, Kampala,*
[1,3]*Uganda*
[2]*Belgium*

1. Introduction

Assessment of climate change impacts on hydrometeorological variables such as rainfall and temperature at regional or local (catchment) scale requires projected future time series. One of the common sources of such future time series are Global Climate Model experiments (GCM runs). However, direct use of GCM runs may not be appropriate for climate change impacts assessment at catchment scale because the scales in GCMs are not at par with the scale at catchment level. For example, if the magnitude of the biases in rainfall and temperature is very high, there is a tendency for the impact signals in the GCM runs to be amplified under very wet and dry conditions (Christensen et al., 2008). Thus, the need for circumventing the biases in or downscaling the GCM runs. Once projected future time series are derived through downscaling, they can either be assessed for impacts by comparing them with the observed or used as inputs into a rainfall-runoff model in order to obtain future streamflow time series. The latter can be compared with the present day control streamflows; hence impacts on streamflows can be assessed. Therefore, methods are needed to downscale output from GCM to represent local climate variables.

Downscaling can be dynamical through the use of an RCM (Regional Climate Model) with output from GCM as the boundary condition (e.g. Christensen et al., 2007) or through statistical (empirical) methods conditioned on large-scale predictors (e.g. Fowler et al., 2007). In most cases, outputs from RCM are also biased and bias-removal (e.g. Piani et al., 2010) is often employed. Often, this method involves some form of transfer function derived from the observed and simulated cumulative distribution functions (e.g. Ines & Hansen, 2006). This method is given a wide range of names in literature such as statistical downscaling, quantile mapping, histogram equalizing and rank matching among others. In applying a hindcast-derived correction to simulations of projected climate, it is assumed that the correction still holds for the projected climate. This is a non trivial assumption (Trenberth et

al., 2003). However, the assumption is more plausible provided the transfer function between the raw and the corrected RCM output is robust. In many regions of the world (e.g. Africa) data limitation will continue to constrain the calibration of RCMs (Anyah & Semazzib, 2007; Christensen et al., 2007) and use of other methods is sought. Bias correction method is sometimes applied to GCM data (e.g. Ines & Hansen, 2006).

In a statistical regression method, a purely statistical relation is sought between a model field that is well-represented on the large-scale (predictor), e.g., sea-level pressure or the height of the 500 hPa level, and the local quantity of interest (predictant), e.g., precipitation or temperature (Benestad et al., 2008). Assuming that the relation still holds in the changed climate, the changes of the large-scale circulation are translated into the local changes that are of interest. Note that the predictant needs not be a variable of the global model, but can be anything related to climate. The great advantage of the statistical method is that it is easy and computationally simple. Nevertheless, (long) time series of both the predictor and the predictant are needed to calibrate the regression model. While the first requirement is usually not a problem, the second limits the applicability of the method to a limited number of places and to surface variables only.

The "delta" downscaling technique uses the concept of change factors (multiplicative or additive) extracted from the climate models and applied to observed time series. The former has been assessed by several researchers (e.g. Diaz-Nieto and Wilby, 2005; Lenderin et al., 2007). The traditional delta technique applies the changes to a time series without considering the variability of the time series. The technique assumes that relative changes obtained from the climate models are more representative than the absolute ones. Furthermore, it is assumed that the biases in the control (present) simulations are similar to the biases in the future simulations. Moreover, the temporal structure of the derived time series is maintained. With significant changesin the variability of time series under climate change the delta method may not be suitable. The earlier attempts to improve on the approach included examining various scenarios (Prudhomme et al., 2002), and applying quantile scaling techniques (Harrold and Jones, 2003) to account for the variability in the time series. Olsson et al. (2009) and Willems and Vrac (2011) demonstrated that deriving future time series that considers changes in extremes is possible through the use of exceedance probabilities. This approach ensures that there is increased variability in heavy rainfall amounts compared to meek rainfall events. This approach is simple, robust and can be applied to any set of data without worrying about the length of a previous record. However, the omission of other changes such as the wet spells, which has very strong association with the extremes in precipitation downscaling, makes the approach further faulty. Accounting for change in wet spells can improve precipitation downscaling and impacts results focusing on extremes.

Previous studies have used and compared different downscaling techniques and have concluded that the choice of the method is dependent on the nature of the study and that more research is needed to improve on available downscaling techniques (Fowler et al., 2007). The tenet of this chapter is centered on the quantile perturbation technique because it is often used to assess the impact of climate change on extremes of the hydrometeorological variable such as precipitation. Improvement of the technique is here suggested and applied to data from a catchment in a tropical climate.

2. Case study

The downscaling technique described in this chapter is illustrated based on a case study of the upper River Nile basin, Lake Victoria basin (Figure 6.1). The River Nile basin (Figure 6.1(a)) is situated between 8°S to 33°N and 20°E to 42°E covering an area of approximately 3,762,000 km² (Figure 6.1(b)). Lake Victoria (Figure 6.1(c)) is the largest fresh water body in Africa and a constituent of the most upper part of the River Nile basin. Lake Victoria is geopolitical in nature and characterized by Kenya, Uganda and Tanzania with Rwanda and Burundi as key sources of the famous River Kagera, the major contributor to the lake Figure 6.1(a). Lake Victoria is, on average, 68,800 km², and is politically shared as follows: Kenya (6%), Uganda (43%) and Tanzania (51%).

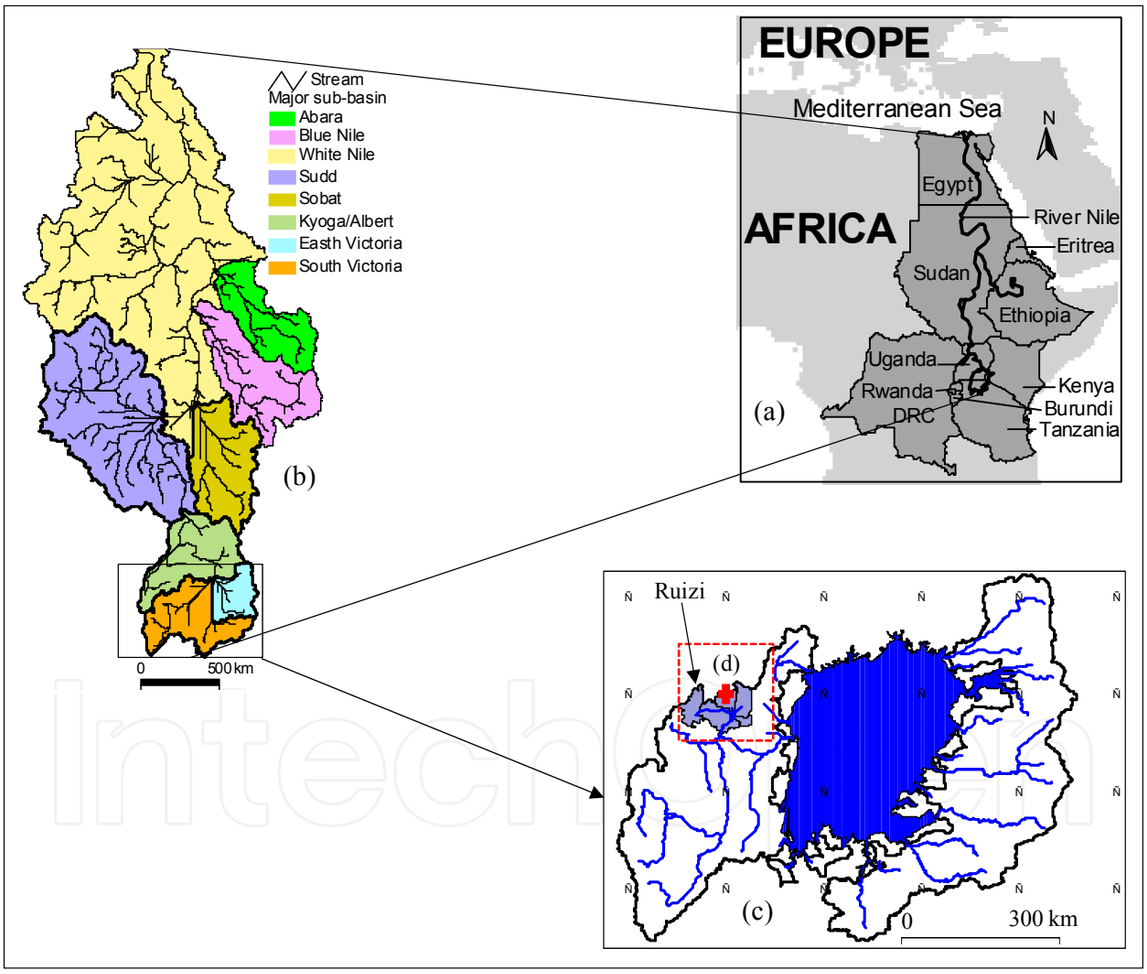

Fig. 6.1. Location of River Nile in Africa, the countries in which the Nile basin takes part (a), the major streams and major catchments of the River Nile (b), the Lake Victoria basin (c) and River Ruizi catchment. The plus (+) signs, superimposed over Lake Victoria basin and River Ruizi catchment indicate the mean grid size of the GCMs used. The dotted square grid with a center at ⧫ indicates the typical GCM grid used in the case study.

The basin area in Uganda is 59,858 km² out of about 196,000 km². Lake Victoria stretches approximately 415 km from north to south; between latitudes 0°30′ N and 3°12′ S and from west to east between longitudes 31°37′ and 34°53′ E. It is situated at an altitude of about 1,130 m above sea level, and has an estimated volume of about 2,750 km², and an average and maximum depth of 40 m and 80 m, respectively. The area of the River Ruizi catchment indicated in Figure 6.1(d) is about 6,000 km² and the observed daily rainfall data of the measuring stations falling within the catchment was used to demonstrate how the GCM data can be downscaled to catchment scale.

3. GCM data

The information of the GCM data (Table 6.1) used here were obtained from the Programme for Climate Model Data Intercomparison (PCMDI) database[1]. The data were used for the Fourth Assessment Report of the Intergovernment Pannel on Climate Change (AR4 IPCC), 2007. There are, however, several public domain databases from which one can obtain either observed climate data and/or climate model data.

Modeling Institution, Country	Center acronym	Model	Model Resolution		Availability of:			
			Lon	Lat	20C3M	A2	A1B	B1
Bjerknes Centre for Climate Research, Norway Norway	BCCR	BCM2.0	2.813	2.791	✔	✔	✔	✔
Canadian Centre for Climate Modelling & Analysis, Canada	CCCma	CGCM3.1(T47)	3.750	3.711	✔	✔	✔	✔
		CGCM3.1(T63)	3.750	3.711	✔	✘	✔	✔
Centre National de Recherches Meteorologiques, France	CNRM	CM3	2.813	2.791	✔	✔	✔	✔
Australia's Commonwealth Scientific and Industrial Research Organisation, Australia	CSIRO	Mk3.0	1.875	1.865	✔	✔	✔	✔
		Mk3.5	1.875	1.865	✔	✔	✔	✔
Max-Planck-Institute for Meteorology, Germany	MPI-M	ECHAM4-OM	3.750	3.711	✔	✔	✘	✔
		ECHAM5-OM	1.875	1.865	✔	✔	✔	✔
Research Institute of KMA, Germany/Korea	MIUB	ECHO-G	3.750	3.711	✔	✔	✔	✔
Institute of Atmospheric Physics, China	LASG	FGOALS-g1.0*	2.500	2.022	✔	✘	✔	✔
Geophysical Fluid Dynamics Laboratory, USA	GFDL	CM2.0	2.500	2.022	✔	✔	✔	✔
		M2.1	2.500	2.022	✔	✔	✔	✔
Goddard Institute for Space Studies, USA	GISS	AOM	3.750	3.711	✔	✘	✔	✔
		E-H	5.000	4.000	✔	✘	✔	✘
		E-R	5.000	4.000	✔	✔	✘	✘
Institute for Numerical Mathematics, Russia	INM	CM3.0	5.000	4.000	✔	✔	✔	✔
Institut Pierre Simon Laplace, France	IPSL	CM4	3.750	2.535	✔	✔	✔	✔
National Institute for Environmental Studies, Japan	MRI	CGCM2.3.2a*	2.813	2.791	✔	✔	✔	✔
Meteorological Research Institute, Japan	NIES	MIROC3.2(h)	2.813	2.791	✔	✘	✔	✔
		MIROC3.2(m)	2.813	2.791	✔	✔	✔	✔
National Center for Atmostpheric Research, USA	NCAR	CCSM3.0*	1.406	1.401	✔	✔	✔	✔
		PCM1*	2.813	2.791	✔	✔	✔	✔
Hadley Centre for Climate Prediction and Research Met Office, United Kingdom	UKMO	HadCM3	3.750	2.750	✔	✘	✘	✘
		HadGEM1	1.875	1.250	✔	✘	✘	✘

Table 6.1. Information on the GCMs and scenarios for the data available at PCMDI. 20C3M is the simulation of the 20th century climate using historical GHG (Green House Gases) concentrations for the period 1871-2000.

[1] The website for PCMDI database is "http://www2-pcmdi.llnl.gov/esg_data_portal", last accessed 13 June 2011.

For its Third Assessment Report, the IPCC commissioned a Special Report on Emissions Scenarios (SRES) which developed about forty different emissions scenarios (Nakicenovic et al., 2000). Of these forty emissions scenarios, six have been chosen as illustrative or marker scenarios: A1FI, A1B, A1T, A2, B1 and B2. Of these six marker scenarios most global climate modelling groups completed climate change simulations using A2, A1B and B1 emissions scenarios in the AR4 IPCC, 2007 (Table 6.2). The choice of the domain is dependent on the purpose for which the climate data is required, the spatial coverage of the data, the temporal resolution, user interest, data completeness and restrictions. The GCM data are coded (mainly in netcdf format, ".nc") and some have quality problems (e.g. error in naming of files, some precipitation values being negatives, etc.). The data were processed and checked for their quality improvements using a cross-pollination of techniques, experiences and tools. For example, CDO (Climate Data Operator) (Schulzweida & Kornblueh, 2011) is a powerful tool for manipulating grid data of different formats. In addition, many other climate data processing tools, such as the NCDF, can be annexed to MATLAB (MathWorks Inc., 2008) and are very instrumental in climate model data processing.

Scenario	Data set	Description	Simulation period	Data available for
20CM3	20th Century simulation	Model input forcings or initial conditions (e.g., solar irradiance, ozone, sulfates, greenhouse gases) are temporally and spatially varied	1870-2000	1961-2000
SRES B1	550 ppm CO_2 maximum (SRES B1)	Atmospheric CO_2 concentrations reached 550 ppm in the year 2100 in a world characterized by low population growth, high GDP growth, low energy use, high land-use changes, low resource availability and medium introduction of new and efficient technologies.	2001-2100	2046-2065 2081-2100
SRES A1B	720 ppm CO_2 maximum (SRES A1B)	Atmospheric CO_2 concentrations reach 720 ppm in the year 2100 in a world characterized by low population growth, very high GDP growth, very high energy use, low land-use changes, medium resource availability and rapid introduction of new and efficient technologies.	2001-2100	2046-2065 2081-2100
SRES A2	850 ppm CO_2 maximum (SRES A2)	Atmospheric CO_2 concentrations reach 850 ppm in the year2100 in a world characterized by high population growth, medium GDP growth, high energy use, medium/high land-use changes, low resource availability and slow introduction of new and efficient technologies.	2001-2100	2046-2065 2081-2100

Table 6.2. Definitions of the SRES scenarios (Nakicenovic et al., 2000).

Although the IPCC (2001a) recommended a 30-year period (1961-1990) as sufficient to measure climate and detect climate change, challenges in climate modelling and archiving of global climate data have forced the global community to consider a 20-year period as plausible for impacts assessment. This is due to the fact that deviation from using a 20-year period from that of using a 30-year period is not very significant. A number of fixed time horizons in the future are considered in literature, especially in the recent AR4 IPCC, e.g., the 2020s (2010-2039), the 2050s (2040-2069), and the 2080s (2070-2099). These are future periods for which any assessment of climate change impacts can be made. Similar to the adjustment of future periods, reference periods have followed suit and quite often studies have adopted 1961-1980, 1971-1990 and 1981-2000. However, in the case where there are

sufficient data, it is strongly recommended that a 30-year period for the current (control) and a 30-year period for the future (scenario) climate be considered.

The GCMs provide area averaged data and this means that for the evaluation purpose, the rainfall measured at a point, for example, requires scaling if areal rainfall measurement is not available. The scaled point rainfall intensity accounts for the expected systematic difference between the point rainfall and the grid averaged GCM rainfall. Point rainfall can be scaled to area averaged rainfall by either applying areal reduction factor (Svensson & Jones, 2010) or by spatial interpolation of point rainfalls using the technique such as Thiessen polygon to obtain areal rainfall. The points (measurement locations) under consideration should all fall within the GCM grid boundary. Thiessen polygon is a preferred method for estimating areal rainfall and was used in this study (Figure 6.1).

Statistics of errors, biases, correlations and trends have been used to quantify statistical inconsistencies between the model simulation and the historical time series. (e.g. Nyeko-Ogiramoi et al., 2010). The bias in the GCMs can not be ignored; especially regarding their selection and application in impact assessment. First, models that are extremely biased can be sieved out of impact assessment. Secondly, the bias in the GCMs means that it is inappropriate to use outputs from GCMs directly for impact assessment at local scale. Furthermore, Christensen et al. (2008) noted that significantly biased models for the current and past climate have potential for transferring significant bias to the future. However, because the pattern of the current and past climate seems to be well represented in the GCM, its pattern prediction (or signal) may be reliable. Conventionally, GCMs are most often assessed for the historical performance alone. However, for a more robust impact assessment, the inter-comparison of the future projections is also vital (Nyeko-Ogiramoi, et al., 2010). This is because models that have good ability in estimating the observed rainfall may not necessarily produce robust predictions (close to or in same direction as other models). Models which perform well for historical periods but are projecting disparate future changes should be further examined for performance. In intermittent variables such as rainfall, the complex climate system may introduce inconsistencies for the future climate. Disqualifying a model, however, from further analysis because it is inconsistent with other models is only vindicated if further examination shows a previously overlooked bias against the observed data (Nyeko-Ogiramoi et al., 2010). The inter-comparison of the projections aims to increase the confidence in the GCM projections while eliminating spurious projections. In addition, the differences in the future projections (controls and projections) if combined with the differences in the current simulation (controls and observation) can enhance the understanding of the effects of the model bias on the future projections. Evaluation studies are valuable as they identify the weaknesses and spot the models whose performance is questionable. The inconsistencies of the AR4 GCMs with the observation over the Lake Victoria basin suggest further tasks for the climate model scientist. That is, further improvements for the GCMs are necessary to increase on the confidence for the assimilation of their outputs. However, the performance of a climate model is regional or catchment based and should be treated as such; the conclusions of performance are mainly valid for the studied area. The models marked with "*" (Table 6.1) are the most biased with respect to rainfall over the Lake Victoria basin (Nyeko-Ogiramoi et al., 2010).

4. Synchrony between wet extremes and wet spells

Analysis of projected changes in climate by Meehl et al. (2007) showed that the type, frequency and intensity of extreme events are expected to change even with relatively small mean climate changes. Meehl et al. (2007) further noted that in a warmer world, precipitation tends to be concentrated into more intense events, with longer periods of light precipitation in between. Thus, intense and heavy downpours would be interspersed with longer relatively dry periods. Furthermore, Meehl et al. (2007) noted that wet extremes are projected to be more severe where mean precipitation is expected to increase and dry extremes are projected to become more severe in areas where mean precipitation is projected to decrease. In concert with the results of projected increased extremes of intense precipitation, even if the wind strength of storms in a future climate did not change, there would be an increase in rainfall intensity (Meehl et al., 2007). Kharin & Zwiers (2005) and Barnett et al. (2006) noted also that the increase in extreme events may be perceived most through the impacts of extremes. The implications are that changes in wet extremes are, quite often, associated with longer wet spells. The need to consider the characteristics of the wet spells is paramount in improving the precipitation downscaling techniques that employ the quantile perturbation approach. Thus, this chapter mainly explores the technique of employing the characteristics of wet spells in and for the improvement of the quantile perturbation approach for downscaling precipiation.

5. Perturbations

In this chapter, perturbation refers to any change that can be obtained from the GCM scenario run in comparison with the control or from the observed time series. That is, the properties (or statistics) of the GCM control run (series) are compared with those of the GCM future series to obtain changes (perturbations) that are projected under the different climate change scenarios. Note that changes that occur in quantitative hydrometeorological variables such as rainfall and evapotranspiration can be obtained in many forms (e.g. ratios, percentage, difference, etc.). Meanwhile, changes that occur in qualitative meteorological variables such as temperature can mainly be derived as differences. Different perturbations for rainfall and temperature time series can be extracted and analysed for different months or seasons and for different GCMs. In the context of this study, emphasis is put on analysing perturbations for daily rainfall because it is an essential variable of climate which is needed for hydrological impacts of climate change. The main principle behind perturbation is that several perturbations can be isolated or extracted from GCM paired (control and scenarios) data at different aggregation levels and can be analysed for their respective properties. In the subsequent sections perturbations for rainfall are analysed for daily rainfall for each month. The results are presented only for the months of January and April for typical illustrations. This is because of the fact that January and April are considered representative of dry season (dry months) and wet season (wet months), respectively, of the climate of the case study.

5.1 Rainfall perturbations

5.1.1 Rainfall wet-days quantile perturbations

Derivation and analysis of rainfall perturbation can be performed for rainfall time series at different time scales. However, in this case, the focus is on a daily time scale and the

perturbations were derived by considering daily rainfall time series for each month, separately. In other words, the time series for each month for all the considered years are pooled together before perturbations are derived. Perturbations are derived only for the wet-day frequency of the rainfall series. The definition of a wet day is given in the next section. If $q_{s1} \geq q_{s2} \geq q_{s3} \ldots q_{sn}$ represent the scenario quantiles and $q_{c1} \geq q_{c2} \geq q_{c3} \ldots q_{qn}$ represents the control quantiles then quantile perturbations are derived as q_{si} / q_{ci}, for $i = 1, 2, 3, \ldots n$. Alternatively, perturbations can be derived as $P_p = Q_{s,p} / q_{c,p}$, where P_p is the perturbation corresponding to probability p, $Q_{s,p}$ is the future scenario value (corresponding to probability p) and $q_{c,p}$ the control value (for the same probability p). The plot of quantile perturbations versus the return period (or exceedance probability) can reveal the effect of projected possible warming for the future.

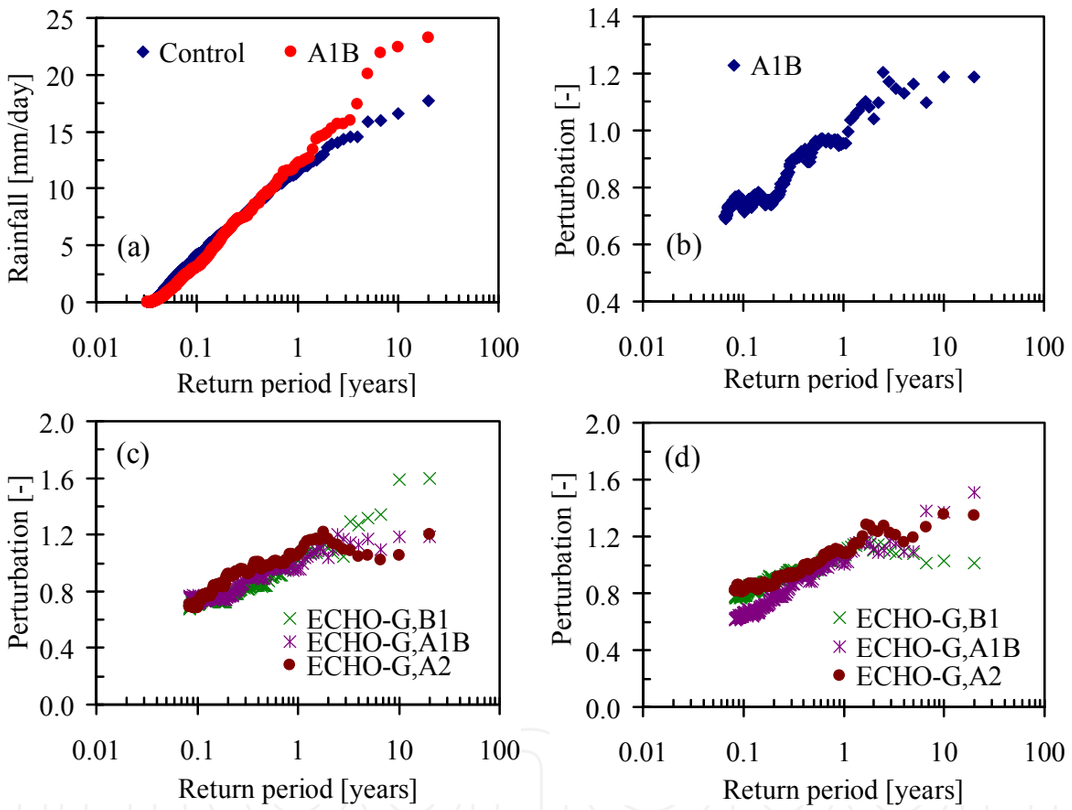

Fig. 6.2. Distributions for January rainfall for control and scenario (A1B) (a), and the corresponding perturbations under A1B scenario (b), and 3 scenarios for periods: 2050s (c), and 2090s (d). The control and the scenarios are for one GCM (ECHO-G) to illustrate the typical perturbations for the two periods. The results are for the GCM data extracted from a grid over the River Ruizi catchment.

Fig. 6.2 shows an illustration of the January daily rainfall distributions for a 20-year period (Fig. 6.2(a)) and the corresponding plot of perturbation versus return period (Fig. 6.2(b)). Perturbations for different scenarios and the corresponding plots for different future scenarios, projected for the periods 2050s (Fig. 6.2(c)), and 2090s (Fig. 6.2(d)), can similarly be obtained. Note that the daily rainfall distribution and the perturbation plots, provided in

Fig. 6.2, represent evolutional stages of rainfall perturbations analysis of an example of one GCM (ECHO)-G). Perturbations analysis for other GCMs can also be obtained and analysed in a similar way.

5.1.2 Dependency of rainfall wet-days quantile perturbations

The effects of climate change on the mild and heavy rainfall events can be exposed by examining the perturbation plot. Such effects can be analysed for different temporal scales such as daily, weekly, monthly and seasonal. For a tropical climate, where the interest of this study lies, the climate is characterized mainly by wet and dry seasons. However, it is important to note that for a given season, daily rainfall variations among the months can be very high. Thus, analysis of perturbations for daily rainfall series for each month is particularly important.

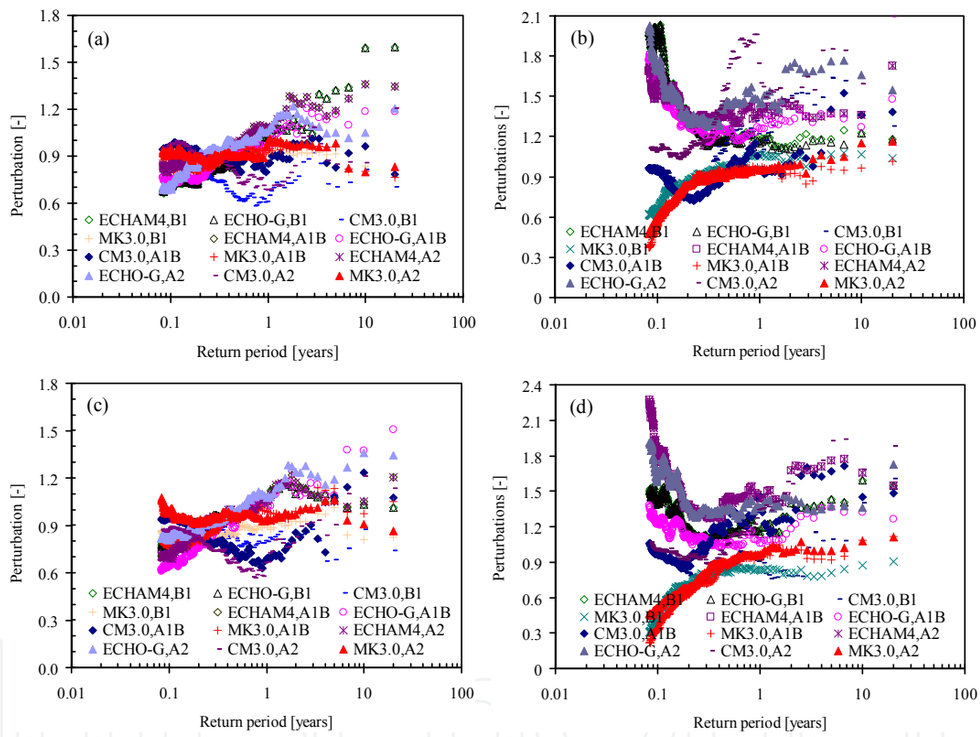

Fig. 6.3. Perturbations for the daily rainfall: (a) January, 2050s, (b) April, 2050s, (c) January, 2090s and (d) April, 2090s. The perturbations are for 4 GCMs to illustrate the typical perturbations for a relatively dry month (January) and a relatively wet month (April). The results are for data extracted from a grid over the Ruizi catchment

Fig. 6.3(a) and (b) shows plots of perturbation versus return period for the months of January and April, respectively, for the period 2050s. For January, the perturbations are generally greater than 1 for the heavy rainfall events (> 1 year). However, the perturbations are less than 1 for lighter rainfall events (< 0.2 years). The perturbations for the mean rainfall events are fairly constant (0.2-0.4 years). It is important to note that for some GCMs (models) the perturbations are less than 1 between 1.1-1.4 years return periods. This variation of the perturbations for the heavy, mean and light rainfall events has implications for the changes

in the rainfall intensity and frequency. First, it is expected that given a rainfall intensity of a return period less than 1 year, the intensity is projected to decrease from the current to the future. Secondly, given a rainfall above one year return period, the intensity is projected to increase from the current value to the future for the most heavy rainfall events. In the latter case, the rainfall intensity for the medium heavy rainfall events is expected to decrease as projected by some GCMs. Thus, for the dry months, the dry days will become moderately dryer and the very wet days will become much wetter. In some cases the frequency of such wetter events will increase.

For the month of April (Fig. 6.3(b)) the perturbations are dramatically higher than 1 for return periods < 0.2 years. This is the case for 9 out of 12 selected GCM runs irrespective of the scenarios. For return periods > 0.2 years the perturbations are generally > 1 but increase with return period moderately. For three models, perturbations are less than 1 for return periods < 1 years. The variation of the perturbations with return period for the month of April has implication for the projected changes in the rainfall intensity and frequency. The rainfall events are expected to strongly increase compared to the current but with moderate increase in their frequencies. Thus, more wet days are projected for the wetter months and the rainfall intensity is projected to increase compared to the current. However, the projections by some models indicate that as the intensity and frequency of the heavy events strongly increase and the magnitude of the mean rainfall events remains constant, the rainfall intensity and frequency of the light rainfall events is projected to decrease compared to the current. In the latter case, it means that lesser amounts of rainfall is projected (dry days becoming dryer) coupled with a decrease in frequency. It is noteworthy, however, that perturbation become very sensitive (very high factors) as the return period decreases and the lighter events for the control series tend to zero. This is particularly important to note because further discussions are given in section 8.1.1.

The differences in the variation of the perturbations for the low (B1), middle (A1B) and high (A2) scenarios, and for the two different future periods 2050s and 2090s, can only be discerned by examining Fig. 6.2(c) and (d) or isolating a case for a model from Fig. 6.3. For return period < 1.1 years, the differences in the magnitude of the perturbations among the scenarios are not very eminent and are consistent for both the 2050s and 2090s. However, for a return period > 1.1 years, the perturbations are eminently different for low, middle and high scenarios and inconsistent for both the 2050s and 2090s. If many models are compared (Fig. 6.3), the differences in the variation of the perturbations for the low, middle and high scenarios become trivial and the intermodal variation becomes fundamental. An important point to note is that perturbations are very sensitive when light rainfall events of very low return periods are considered. That is, the values of the perturbations can be dramatically low or large for meek events with intensity close to naught. In the latter case, it is recommended to derive perturbations while considering only the days above a certain-carefully-selected threshold intensity value or particularly wet days which buffers the sensitivity of the perturbations.

5.1.3 Wet days and wet-days frequency perturbation

Schmidli & Frei (2005) defined wet days as the annual count of days with daily precipitation greater than or equal to a certain threshold precipitation value (e.g. ≥ 1 mm). In contrast, dry days are defined as the annual count of days with daily precipitation less than a certain

threshold precipitation value (e.g. < 1 mm). Thus, wet days of a given month can be defined as the monthly count of days with daily precipitation greater than or equal to a certain threshold precipitation value (e.g. ≥ 1 mm or ≥ 0.1 mm). Given the fact that the frequency and intensity of precipitation are projected to change, as learned from the perturbations of rainfall intensity, wet days are also projected to change and it is possible to obtain wet-day frequency perturbations and analyze its variation for the different scenarios and models. Thus, the monthly wet-day frequency perturbation is, hereafter, simply referred to as wet-day perturbation. The wet-day perturbation is calculated as the ratio of the projected (scenario) total number of wet days to the corresponding total number of wet days in the control period and can be calculated as follows:

Let $(X_p)_{i,m}$ be the model daily time series of a given month, m, corresponding to the control of the p^{th} GCM, $p \in \{1,\ldots,M\}$, M is the number of control simulations or the GCMs, and let $(Z_{p,s})_{i,m}$ be the model time series for the projected scenario, s, $s \in \{1, \ldots, W\}$, where W is the total number of projected scenarios, for $i = 1, 2,\ldots, n$, and for month $m = 1, 2, \ldots, 12$. Note that n is the total number of years of the model simulations. If, $t_{c,m}$ is the threshold rainfall intensity for a given month, m, the wet-day perturbation is given by

$$\Delta d_{p(m)} = 100 * \left(\frac{d_{p(s,m)} - d_{p(c,m)}}{d_{p(c,m)}} \right) \tag{6.1}$$

where, $\Delta d_{p(m)}$ is the projected percentage change in wet-day for a given month, m, $d_{p(s,m)}$ and $d_{p(c,m)}$ are the respective total number of wet days with intensity > $t_{c,m}$ in scenarios and control. Note that the control and future periods considered are 1971-1990 (Control) and 2045-2065 (2050s) and 2081-2100 (2090s), respectively. Thus, n = 20 years.

Fig. 6.4 shows the wet-day perturbations for 16 GCM runs for high, middle, and low scenarios and for two different projected future periods (e.g. A2, 2050s for Fig. 6.4 (a)). For the months of January-May the wet-day perturbations are generally > 1 but < 2. In contrast, the wet-day perturbations are also generally > 1 for the months of October-December but > 2 for some models. Meanwhile, for the months of June-September the wet-days perturbations are generally < 1. It can further be seen that the perturbations, for the months of April-May and October-November; are relatively higher for the months where perturbation values > 1. Also for the months where perturbations < 1 its values for the months of June-August are relatively lower. Note that the wetter months are April, May, October and November; and the drier months are mainly June-August. Thus, the implications of the differences in the perturbations for the different months are that the wet days in the wet and dry seasons are projected to increase and decrease respectively in the future. The increase in the wet days will vary with the high, middle, and low scenarios. The high scenario (first row of charts in Fig. 6.4) reveals more increase in wet days than the middle scenario (second row of charts in Fig. 6.4); and middle scenario (second row of charts in the Fig. 6.4) reveals more increase in wet day than for the low scenario. If the charts in left column (for 2050s) and the ones in the right column (2090s) of Fig. 6.4 are compared, it can be seen that the increase and decrease in the wet days for the wet and dry seasons, respectively, are projected to be relatively higher for the 2090s than for the 2050s.

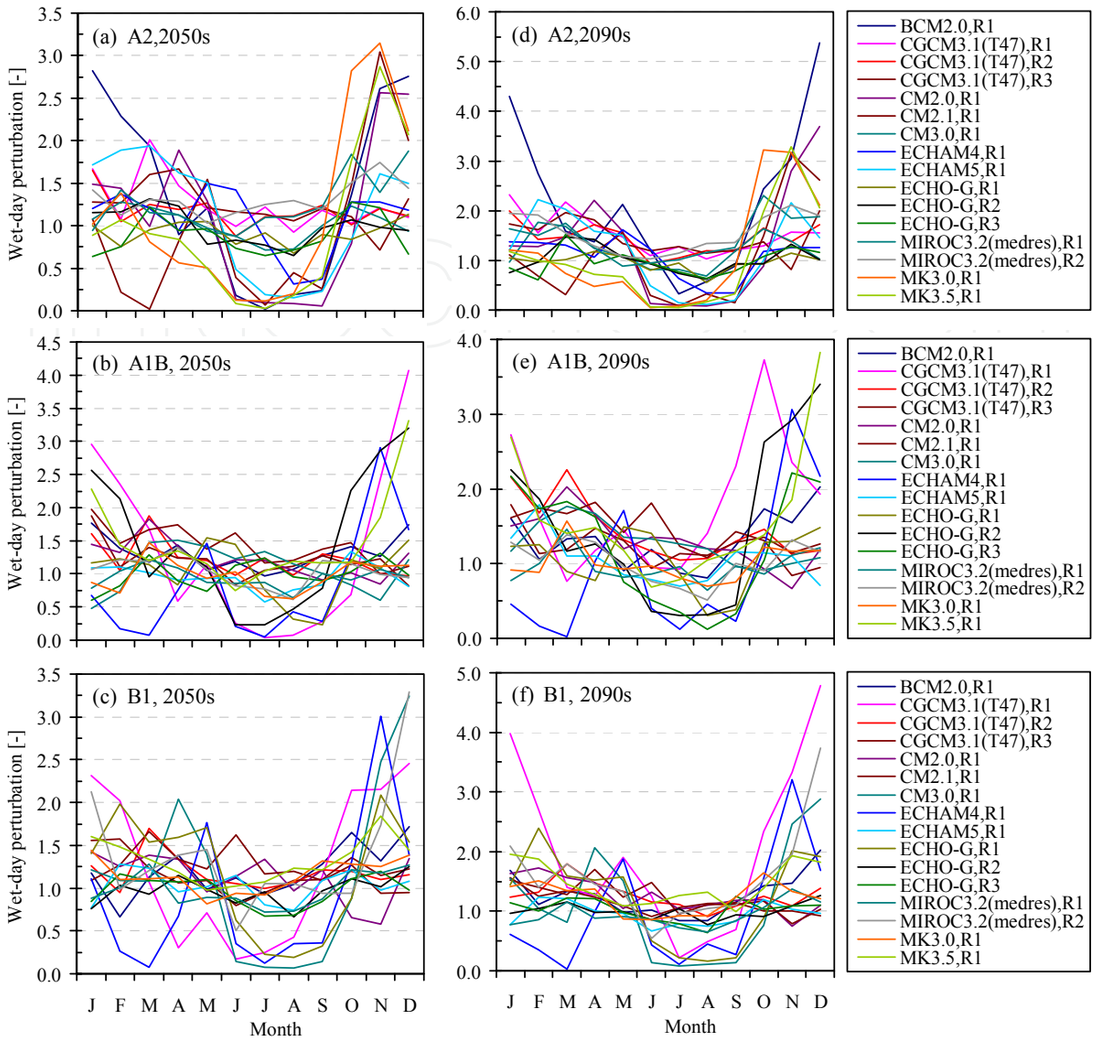

Fig. 6.4. Typical monthly wet-day perturbations for GCM runs calculated for a grid over the Ruizi catchment.

5.1.4 Wet spells and mean wet-spell perturbation

A wet spell is defined as the number of consecutive wet days in a time series in which precipitation intensity exceeds a certain threshold precipitation value (Lall et al., 1996). The length of a wet spell is measured in days.

Wet spells are considered to be one of the most important indicators of extreme precipitation indices. The basic indices of wet spells include, but are not limited to: (1) the maximum number of consecutive wet days in which the total precipitation is greater than or equal to a certain amount, and (2) the mean wet-spell length (mean wet spell), which is the average length of the wet spells in a month, season or year (Schmidli & Frei, 2005). These indices represent characteristics of the duration of consecutive wet-day sequences (Schmidli & Frei, 2005). The latter is particularly of interest to this study. Analysis of the projected

changes in wet spells provides insight into how the future rainy days, as projected by the climate models, will be like. As established in the analysis of the wet-day perturbations that the wet days are projected to change, it is important to assess how the increase in the wet days, for example, affects the mean length of wet spells. Study by Yue-Cong and Barry (2010) on how climate change may influence the demand for water in the future under different climate change scenarios, showed that changes in wet spells will have significant implications for water supply.

Given a GCM run (control and scenarios) and if 1 mm/day is the threshold precipitation that define a wet day in the control run ($t_{c,m}$), then the mean wet spell for a given month can be obtained. Similarly, the corresponding mean wet spell for the scenario is also calculated based on $t_{c,m}$. This procedure can be repeated for all the months, scenarios, and for all the considered GCMs as well as for the periods under consideration. Fig. 6.5 shows an example from one GCM run under the high, middle and low scenarios for periods 2050s and 2090s to illustrate the typical mean wet spell in control and scenario.

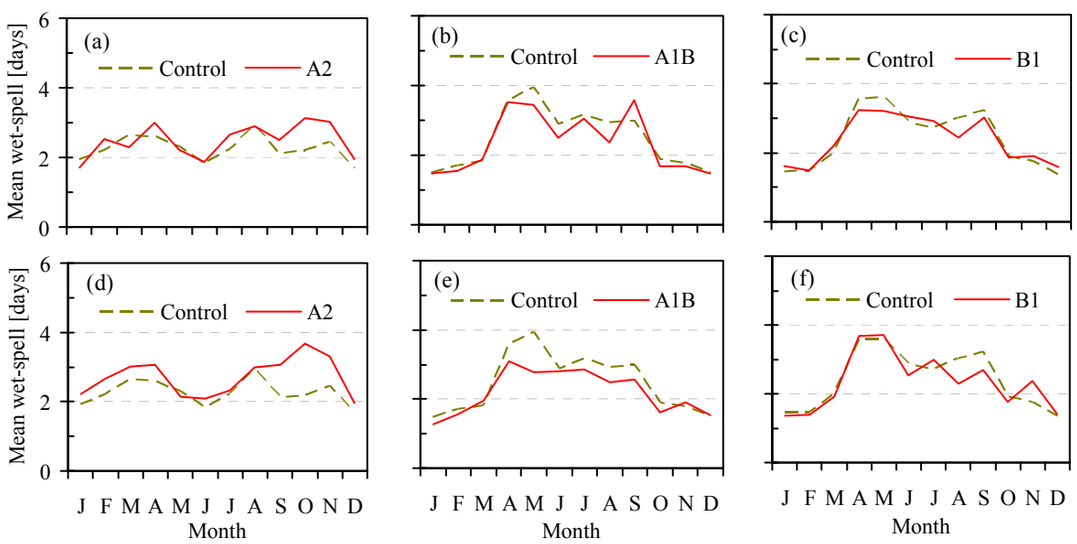

Fig. 6.5. Typical monthly mean wet-spell length for rainfall data of a GCM (MIROC3.2(medres),R1) run calculated for a grid over the River Ruizi catchment for the periods: (a)-(c) 2050s, and (d)-(f) 2090s.

It can be seen that, under the high scenario (2050s), the mean wet spell for the months of January and March is projected to decrease with respect to the present whereas for the months of February, April, July and September-December it is projected to increase also with respect to the present (control) (Fig. 6.5(a)). Fig. 6.5(d) shows that the increase in the mean wet-spell for the months of March-April and September-November will relatively be higher.

The implications are that the increase in mean wet spell for the wet months is probably a manifestation of longer wet spells under the high scenario. Also the increase in the mean wet spell in the 2090s will be higher than that in the 2050s under the high scenario. Under the middle scenario (Fig. 6.5(b) and (e)), the plots for the scenario lie below that of the control run for both the 2050s and 2090s mainly for the very dry (June-August) and very wet

months (April-May). This implies that the GCM run generally projects a decrease in mean wet spells for both the very dry and very wet months with a relatively no change for the other months. The model, under low scenarios, however, projected little change (Fig. 6.5(c) and (f)).

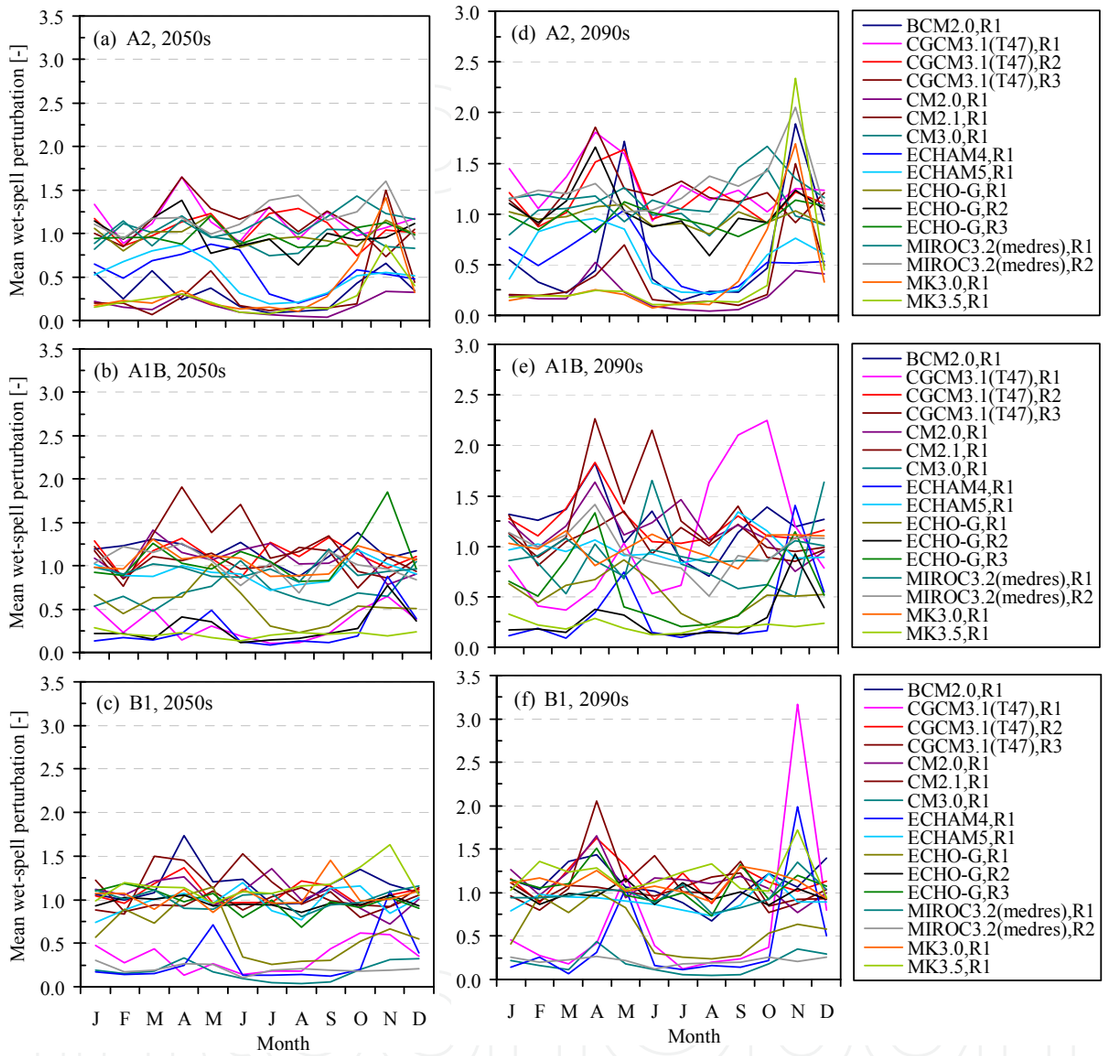

Fig. 6.6. Typical monthly mean wet-spell perturbations obtained from daily rainfall of 16 qualified GCM runs extracted from a grid over the River Ruizi catchment.

Perturbation of mean wet spell is calculated as the ratio of the mean wet spell for the scenarios series to that of the control and can easily be represented in terms of percentage. If $w_{p(s,m)}$ and $w_{p(c,m)}$ is the mean wet spell for scenario and control series, respectively, the mean wet-spell perturbation is given

$$\rho_{p(m)} = \left(\frac{w_{p(s,m)}}{w_{p(c,m)}} \right) \tag{6.2}$$

where $\rho_{p(m)}$ is the mean wet-spell perturbation and the equivalent percentage change is given by

$$\Delta\rho_{p(m)} = 100 * \left(\frac{w_{p(s,m)} - w_{p(c,m)}}{w_{p(c,m)}} \right) \tag{6.3}$$

Fig. 6.6 shows monthly mean wet-spell perturbations of 16 model runs under high, middle and low scenarios for the 2050s and 2090s. It can be seen that there is a "band of plots" with mean wet-spell perturbations that resonates around 1, with some completely below 1 and some, for the month of November, willowing out (Fig. 6.6(a)). A similar pattern of the former can be seen in Fig. 6.6(d) but with a shift in the upper "band of plots". Fig. 6.6(d)-(f) further shows that for models with mean wet-spell perturbations < 1, the mean wet-spell perturbations are generally < 0.5 for most models, except for the months of May and November. Similarly, Fig. 6.6(d)-(f) also shows that for the models with mean wet-spell perturbations > 1 the mean wet-spell perturbations generally lie in the range 1-1.25 except for the months of April and November. Fig. 6.6(a)-(f) also reveals that the mean wet-spell perturbations for the months of February and August < 1 for most models. It can be seen also that the "depression" in the plots for models with mean wet-spell perturbations < 1 is eminent for the months of June-September. The preceding discussions have implications for the changes in the wet- and dry spells. First, the mean wet spell for the wet seasons is projected to increase and the wet spells for the wetter months will increase more than that for the less wet months. Secondly, for dry season where the mean wet spell is projected to decrease, the wet spells in the drier months will decrease more than that in the less dry ones. Furthermore, the change in the mean wet spell implies that the distributions of both the wet- and dry spells will alter.

Fig. 6.7 shows the distributions of the wet/dry spell lengths for the months of January and April. The ordinates and the abscissa of the plots (Fig. 6.7) represent the relative frequency (pmf) and the days, respectively. It can be seen that the proportion of wet spells with length of one day is projected to reduce and the proportion of wet spells of length 2 days will dominate (Fig. 6.7(a)). Meanwhile the proportions of wet spells of length 2-3 days will reduce in the future. Wet spells of length greater than 4 days are projected to increase. The implication of the latter is that increase in the frequency of longer rainy days may be linked to river flooding. Fig. 6.7(c) shows that, generally, the proportion of the dry spells will reduce for the dry months. Fig. 6.7(c) shows that the proportions of wet spells of length between 3-10 days will increase and this means that the current longer wet spells are projected to be longer. For both the dry and wet months the wet spells of length 4-10 days are projected to increase. Thus, the frequency of wet days and dry days are projected to increase and reduce, respectively. Furthermore, the increase in the mean wet spell may be a manifestation of the increase in the longer wet spells.

Note that perturbations of the mean and coefficient of variation of the intensity for the wet days can also be obtained by comparing the one of the scenarios to that of the control. This enables analysis of the possible change in the mean and also the variability of the wet day intensity as a result of the influence of climate.

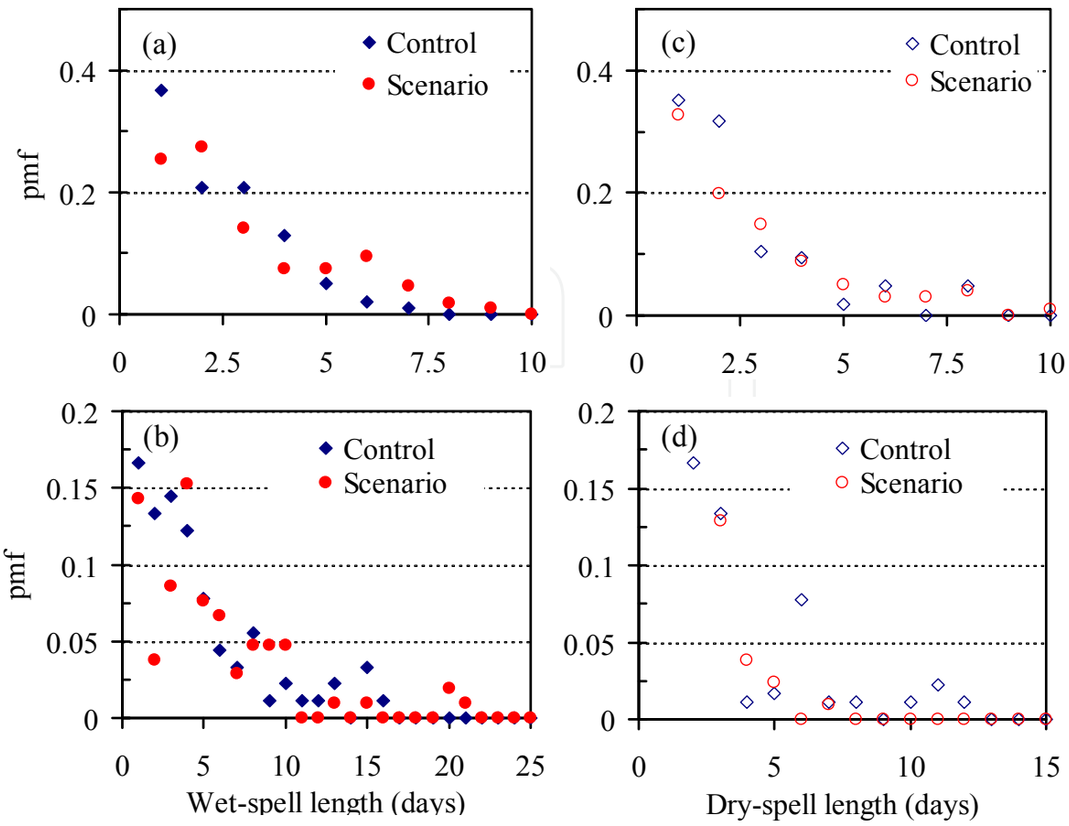

Fig. 6.7. Typical distributions for: (a)-(b) wet spells, (c)-(d) dry spells for: (a) and (c) January, and (b) and (d) April for an example data set for a GCM run (CGCM3.1(T47),R2) under A2 scenarios, 2090s, extracted for a grid over the River Ruizi catchment.

6. Climate change signals

We refer to perturbations extracted from GCM control and scenario runs, such as for rainfall intensity, wet-day, mean wet-spell, mean and C_v of the daily rainfall for each month as climate change signals (CCS). If we assume that the bias in the control runs is similar to the bias in the scenario runs then CCS are bias-free. Transfer of the CCS to observed time series (OS) at local scale would thus produce perturbed observed series (POS) which have similar statistical properties as the projected future time series. In the context of this study, we refer to the process of transferring the CCS to OS as a nonparametric statistical downscaling of GCM runs based on adaptive perturbation approach. The procedure for transferring the climate change signals is discussed in section 8.0

7. Conclusions on perturbations and climate change signals

The change (perturbation) between GCM scenario and control runs provides useful information on climate change signals in the hydrometeorological time series. Such climate change signals if carefully extracted can provide substantial preliminary information on climate change impacts assessment at local scale. A methodology that can transfer CCS to OS at local scale with minimum error margins would constitute an important nonparametric

statistical downscaling of GCM runs. The resulting downscaled time series can be used in hydrological climate change impacts at local scale.

8. Perturbation approach for statistical downscaling

The CCS, considered important for capturing change, can be transferred to OS using a perturbation approach without explicit assumption of the underlying distribution to obtain POS. A number of nonparametric approaches are used in stochastic hydrology to generate weather variables (Lall, 1995). An approach is considered nonparametric if (1) it is capable of approximating a large number of target functions, (2) it is "local" in that estimates of the target function at a point use only observations located within some small neighborhood of the point, and (3) no prior assumptions are made as to the overall functional form of the target function. In the perturbation approach, some CCS is used to perturb OS to obtain POS such that the other CCS are used to validate POS. Once POS is obtained and validated it can be employed in climate change impacts assessment at local scale.

8.1 Application to rainfall

In the downscaling of the daily rainfall time series, two CCS are considered: (1) wet-day rainfall intensity perturbations, and (2) mean wet-spell perturbations, as the most important signals to transfer to OS. The mean and the coefficient of variation of the wet-spell rainfall intensity, the mean wet-spell and the distributions of the wet-spells are the statistics used in the validation of POS. In the following sections we discuss how each of the selected CCS are transferred and validated.

8.1.1 Wet-day climate change signals

The wet-day intensity perturbations (perturbation factors) are calculated based on the procedure described in section 5. However, a methodology for choosing a threshold intensity value that defines a wet day in the GCM control series (CS) is revised by involving OS. Let t_o be the threshold wet-day rainfall intensity selected to define a wet day for OS. The corresponding wet-day rainfall intensity value for CS, t_c, is the value that makes the number of wet days in the OS equals the number of wet days in the CS, provided CS is positively biased. If CS is negatively biased, the value of t_c is taken to be the same as t_o. This is to ensure that all the wet days' properties for OS, POS, CS and scenarios series are correctly estimated and to eschew "chaos" from wet-day intensity perturbations with low return periods. For example, if the GCM is positively biased and t_o = 1 mm, $t_c > t_o$ (e.g. t_c = 8.2 mm). Thus, all the properties of the wet days in both the CS and the GCM scenario series (SS) are calculated by considering the value of t_c. Fig. 6.8 shows an example of the threshold wet-day intensity values for 16 different CS for all the months compared against t_o = 0.1 mm of an observed time series. It can be seen that the CS can be highly and positively biased with, for example, 0.1 mm in observed time series being simulated to be 16 mm in the CS.

The values of the wet-day intensity for the OS are ranked and the exceedance probability of each data point is calculated based on its rank number. Similarly, the values of the wet-day intensity for SS are ranked and the exceedance probability of each data point is calculated

based on its rank number. The perturbation is therefore the ratio of the wet-days intensity for SS to that of CS with same probability. Note that if the SS has more wet days than the control, the exceedance probability points are also more than that of the CS and OS. Thus, the perturbations of the extra wet-days intensity values in the SS are obtained by interpolating over the wet-day intensity values for CS. The perturbations are then applied to the wet-day intensity for the OS to obtain POS. In the case where more wet days are projected by the SS the extra wet day perturbations are also applied to the wet-day intensity values interpolated over wet-days intensity values for OS. Note that this methodology ensures that the extra wet days (projected increase in wet days) are added during the application of perturbation factors to OS. If the GCM projects decrease in the number of wet-day then the wet-day intensity perturbations are only applied to the OS based on exceedance probability "equation" and the extra wet days in the OS are converted to dry days. Figure 6.9**.** (a) and (b) shows the wet-day intensity before and after application of perturbations, respectively.

The procedure described above is carried out for each month but for all the years of the time series record. The POS is then resorted to enable transfer of CCS for the mean wet spell. The properties or the statistics of the resulting POS are compared with the statistics of the OS to obtain climate change signal at local scale (CSL).

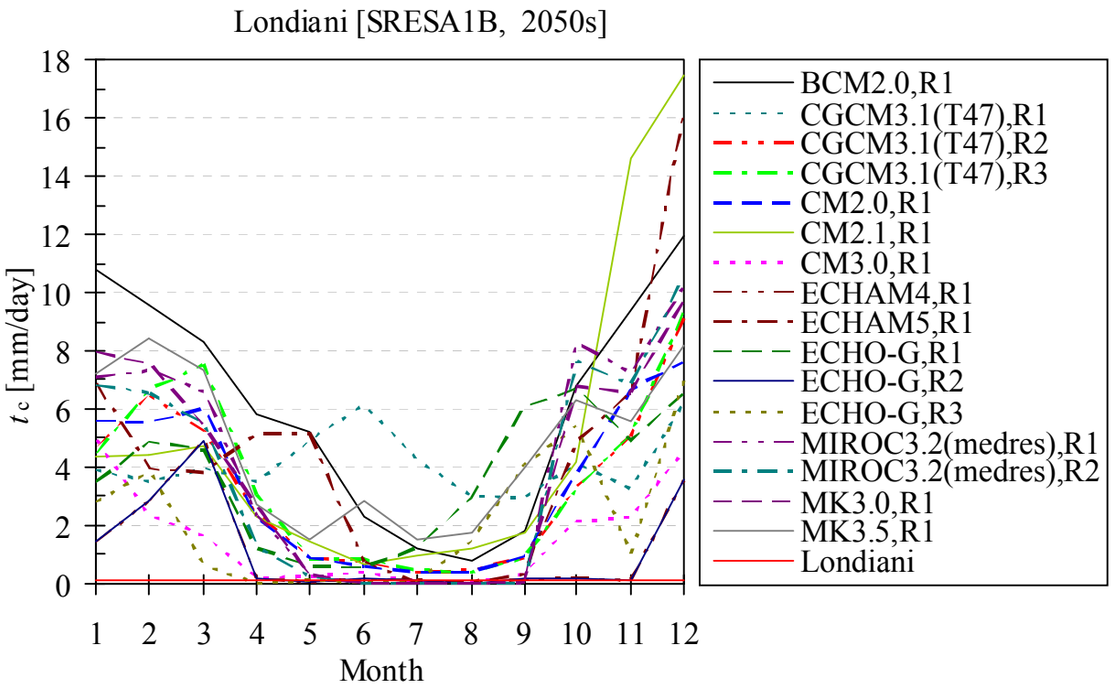

Fig. 6.8. Typical threshold for monthly wet-days daily intensity for different CS compared to t_o = 0.1 mm for an observed time series (Londiani) for a GCM grid over the River Ruizi catchment.

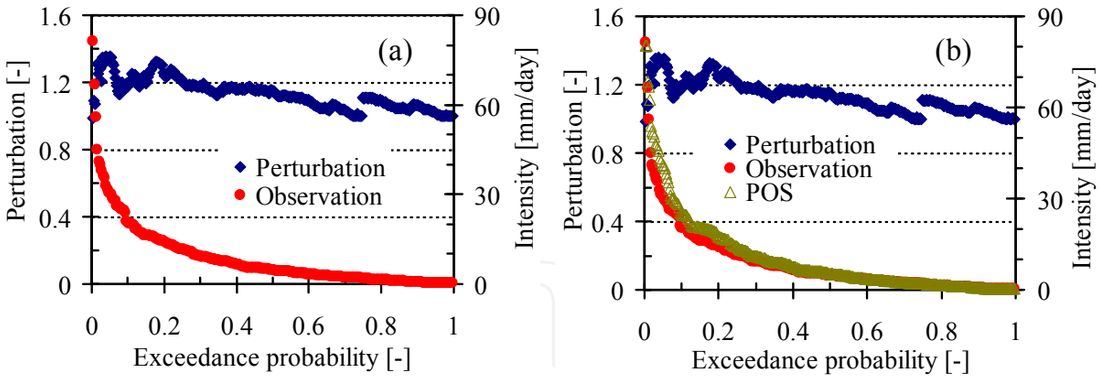

Fig. 6.9. Typical wet-days daily rainfall intensity for the OS before (a), and after (b), application of perturbations. The OS is the areal rainfall data over Ruizi catchment and the GCM data is extracted from a grid superimposed over the River Ruizi catchment.

8.1.2 Wet-spell climate change signal

The transfer of the mean wet-spell perturbation is only considered after the perturbations of wet-days intensity. The wet spells to be adjusted are those in POS. There are only two cases of change to be considered in the mean wet spell: an increase or a decrease in the mean wet spell. In the case of an increase in the mean wet-spell, each of the wet spells in POS greater than their mean value is adjusted by the mean wet-spell perturbation. That is, each of the wet spells in POS greater than their mean value is extended by giving it additional wet days. The value(s) of the wet-day intensity to be added, in order to extend a wet spell, is/are obtained through a non-parametric resampling technique using kernel density estimates (Lall et al., 1996, also see next section). For the case of a decrease in the mean wet spell, each of the wet spells in POS greater than their mean value is reduced by the mean wet-spell perturbation. The reduction of each of the wet spells with length greater than their mean value is carried out by extending the dry spells bounding the target wet spell. That is, extra wet days in the target wet spell are converted into dry days by removing the required number of wet days located at the ends of the wet spells and replacing them with dry days. The statistics of POS are calculated and compared with the statistics of OS to obtain adjusted climate change signal at local scale (CSLa). CSLa is validated against CCS and if the error margins are small enough, the modified POS (POSa) is the downscaled GCM run which represents the projected time series at the local scale.

Note that the wet days to be added are considered days with missing value(s) and is/are added at the ends of the target spells in a proportional way. That is, the wet and dry spells are assumed to be independent where no transition to the same spell is possible. The application of wet-spell perturbation to OS, in downscaling GCM runs, is similar to the nonparametric approach used for generating weather variables in which the wet/dry spell approach is used. There are two major advantages of considering perturbation of wet spells in the perturbation approach for downscaling GCM runs. First, compared to the quantile perturbation approach by Ntegeka (2011), the rainfall spell structure, in the OS and the change in the mean of the OS wet spells lengths, as projected by GCM, are both considered concurrently. This makes it an improvement and advancement of the quantile perturbation approach by Ntegeka (2011) where only the wet-day frequency and wet-day rainfall

intensity are considered. Secondly, the distribution of the spells can easily be validated against that of the GCM. That is, the distribution of the spell change signal can be checked graphically. However, as noted by Lall et al. (1996) the justification of the independence between the wet and dry spell lengths at short time scales is difficult. Nevertheless, the data are allowed to inform the wet spells perturbation process to ensure that very long wet spells, separated by a very short dry spell, are not merged.

8.1.3 Kernel density estimation method

Kernel density estimation is a robust nonparametric way of estimating the Probability Density Function (PDF) of a random variable. The technique does not assume any functional form of the PDF and allows its shape to be entirely determined from the data. The paper by Lall et al. (1995) presents a comprehensive nonparametric approach to a stochastic model for generating daily precipitation based on Kernel density estimation. The salient features of the model were the consideration of the alternating wet/dry spells of a daily rainfall structure within the wet spells. Kernel density estimates (k.d.e) were espoused as effective methods for recovering univariate, multivariate (conditional), discrete and/or continuous probability densities that were directly required from the histogram record. Furthermore, in Lall et al (1996), kernel density estimators of continuous and discrete variables were critically reviewed and tested with various data sets. The k.d.e methods have garnered favours for generating weather time series for various applications with Rajagopalan et al. (1997), and Rajagopalan & Lall (1999) expanding the methods to "*k*-nearest neighbours resampling". Lall et al. (1996) stated that sampling from k.d.e., compared to sampling from the empirical distribution of the data itself, can lead to a reduced variance of the popular Monte Carlo design. The aim here is to take advantage of the flexibility and robustness of the kernel density estimator for generating daily precipitation from which it can be resampled to extend the wet spells in POS. The normal kernel (Lall et al., 1996) is a robust estimator and is often recommended for use when dealing with real-valued random variables that tend to cluster around a single mean value and was used in this study.

8.1.4 The overall flow chart for the downscaling

The downscaling process applied in this study involves the following seven steps. (1) Choose the threshold intensity that defines a wet day from OS and obtain the corresponding value that defines a wet day in CS and SS. Select and calculate the CCS from CS and SS needed for perturbation. (2) Calculate the wet-day intensity perturbations from CS and SS by considering rainfall quantiles with same exceedance probability. Note that the exceedance probability is calculated based only on the wet days. If there are more wet days in SS than in CS, the additional quantiles for CS are obtained by interpolation over its ranked series. (3) Modify each of the OS quantiles by wet-day intensity perturbation to obtain POS. Note that additional wet days are added through interpolating over OS for additional quantiles and are modified by the extra perturbation factors obtained in step (2). (4) Calculate CSL and validate them against CCS obtained in step (1). (5) Transfer the mean wet-spell perturbation through extending or reducing the length of each of the wet spells greater than their mean value. Use k.d.e to generate intensity values from which you can sample to extend the required wet spells. (6) Calculate the new CSL after application of the wet-spell perturbation (CSLa) and validate it against CCS. If the respective errors between

CSLa and CCS are small enough then the final POS is POSa (POS modified by wet-spell perturbation), if not, repeat step (5)–(6). (7). Examine the distribution of the wet spells graphically for visual satisfaction.

8.1.5 Validation of results

The key aspect in the wet-spell technique of the perturbation approach for downscaling GCM runs to local scale is the validation of the climate change signals. Four important characteristics of a rainfall time series for deriving climate change signals needed for the validation of the results are: (i) mean wet-day daily intensity, (ii) mean monthly volume of the wet-day intensity, (iii) mean wet spell and (iv) coefficient of variation of the wet-day intensity. This section presents an example of one GCM to illustrate the typical validation results.

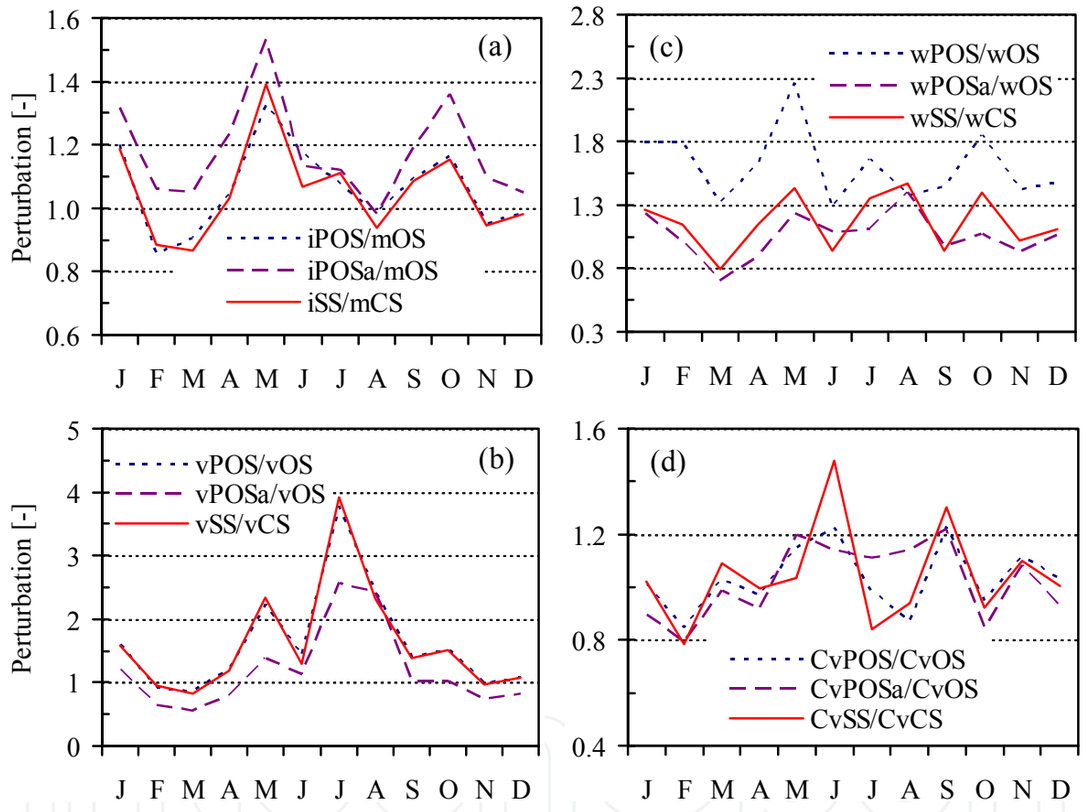

Fig. 6.10. Typical validation results for the climate change signals: (a) mean wet-day daily rainfall intensity, (b) monthly mean volume for the wet-day rainfall intensity, (c) mean wet-spell length, (d) coefficient of variation for the wet-days daily rainfall intensity for an example GCM run (CGCM3.1(T47), R2). The results are for the data extracted from a GCM grid over the River Ruizi catchment.

Fig. 6.10 shows the validation results for the selected climate change signals. The perturbation represents the change or ratio of the time series feature between the control and the target series for the different months. The plots represented by continuous dot and dash lines are for CCS(xSS/CS), CSL(xPOS/OS) and CSLa(xPOSa/xOS), respectively, where x represents the time series feature or statistic under consideration. The time series features, $x = i, v, w, C_v$,

represent intensity, volume, mean wet spell and coefficient of variation, respectively. It can be seen that application of wet-day intensity and wet-day frequency perturbations to OS can perfectly transfer the CCS for intensity and volume (Fig. 6.10(a)-(b)). In addition the change in variability (C_v) is also well transferred simply by applying wet-day intensity and wet-days frequency perturbations (Fig. 6.10(d)). However, the transfer of wet-day intensity and wet-day frequency perturbations alone do not "honor" in any way the CCS for the wet spells except or perhaps by chance (Fig. 6.10(c)). Fig. 6.10(a) and (c) reveals that application of wet-day intensity and wet-day frequency perturbations to OS alone results in a perturbed observed series which has "inflated" mean wet spell above the one projected by the climate model. Fig. 6.10 (a)-(b) indicates that adjustment of POS series to reflect change in the spells, as projected by the model, results in the reduction of the volume of the time series, especially in the case where the model projected decrease in the mean wet spell. However, the reduction in the mean wet-day is an indication that the mean wet-days intensity will increase (Fig. 6.10 (a)). In general, Fig. 6.10 shows that the mean wet spell is projected to reduce but the intensity of the rainfall will increase. The latter is projected to influence variability in the intensity and volume of rainfall for the very dry months or season (June-August).

(a) Distribution of wet spells

Figure 6.11 (a)-(b) shows the distribution of the wet spells for the months of January and April. The ordinate represents the relative frequency or the mean proportion of the wet spell of a given length (1-10 days) in that month in a period of 20 years. Figure 6.11**.** (c)-(d) shows the change in the distribution of the wet spells. From Figure 6.11.(c)-(d) it can be seen that application of the perturbation for the mean wet spell substantially improves the distribution of the wet spells in the POS. Furthermore, it can be seen from Figure 6.11. that there are more wet-spell events with length < 3 days for the month of January compared to that of April which has less wet-spell events of length less than 3 days. The wet spells with length 3-5 days dominate the wet-spell events for the month of April. Figure 6.11. shows that the proportions of wet spells of length 5-7 days for January, and 4-7 days for April, are projected to increase for both the months of January and April. Taking into account that intensity is projected to increase; the increase in longer wet spells has implications for the land areas with very high runoff coefficient and poor drainage. The longer wet spells events may have some influence on flooding than shorter ones. Note that, albeit the changes in the distribution of the wet spells of several GCM runs were analyzed, for both for the period 2050s and 2090s and also for different observed data, the results presented here are not in any way exhaustive.

(b) Distribution of rainfall series

Fig. 6.12 shows the distribution versus retrun period for the daily rainfall for eight different months. Generally, it can be seen that the rainfall intensity with lower exceedance probability are projected to increase more than those with higher exceedance probability. Also, it can also be seen from Fig. 6.12 that generally the intensity of POSa, with exceedance probability between 0.08 and 0.1, will not change so much from that of OS. However, from Fig. 6.12(b), (f) and (h), it can be seen that the distributions for the POS for the mean events are above that of OS. This implies that application of intensity and wet-day frequency perturbations alone without considering perturbation for the mean wet spell results in, probably, overestimation of the mean rainfall events (also see Fig. 6.2). Consider Fig. 6.12(b)-(c) and given an exceedance probability less than 0.08; projected distributions for POS and POSa lie above the distribution

of OS. Similarly, the distributions for POS and POSa lie below the distribution of OS for exceedance probability > 0.1. These changes imply that the values of the intensity for the mild events are projected to decrease and that for heavy events are projected to increase for that month. Fig. 6.12(f)-(h) also shows similar changes. Thus, the mean of the wet-day intensity will increase for the wet months, which is consistent with the results of the increase in the mean of the wet-day intensity shown in Fig. 6.10(a).

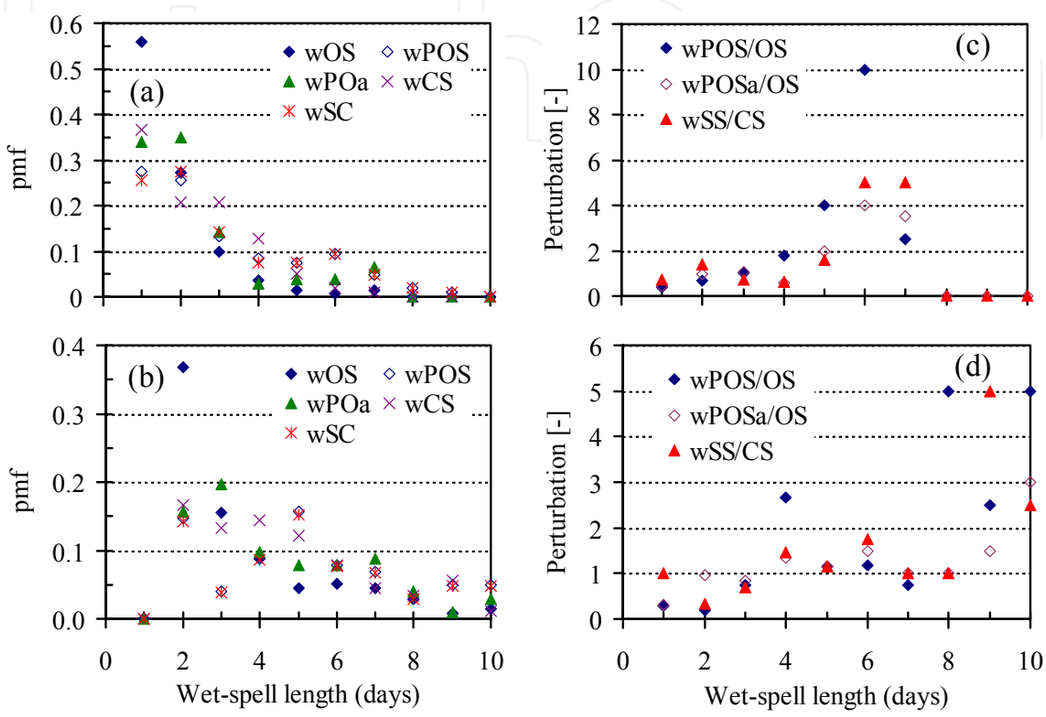

Fig. 6.11. Typical validation results for the wet spell distribution: (a)-(b) January (b)-(c) April for an example GCM run (CGCM3.1(T47), R2). The results are for the data extracted from a GCM grid the River Ruizi catchment.

However, Fig. 6.12(a) shows that the intensity for both the mild and heavy events will decrease. In contrast, Fig. 6.12(e) shows that the intensity of both the mild and heavy events will increase. Further more, Fig. 6.12(d) shows that the intensity of the medium events will decrease and the intensity for the heavy events will increase. Thus, for the dry months consistent change pattern is not eminent. Fig. 6.13(a) shows the distributions for OS, POS and POSa. Meanwhile, Fig. 6.13(b) shows the original perturbations derived from control and scenarios and that which is derived from observed and the downscaled series for the month of January. Fig. 6.13(a) can be compared with that of similar plot for CS and SS (e.g. Fig. 6.2(a)). Note that the result is for the same model and same scenarios (ECHO-G). It can be seen that the distributions for OS and POSa follows similar change pattern as the distributions for CS and SS. This may suggest that Fig. 6.10(a) gives a false impression of a perfect match when *i*POS/*m*OS iSS/*m*CS are compared. Fig. 6.13(b) shows that the actual perturbations needed to be transferred to the OS is not the same as that derived from CS and SS if the change in wet spells is to be considered. In the latter case, the perturbations for intensity with heavy events are actually higher and those for mild events are lower if change in wet spells is taken into account.

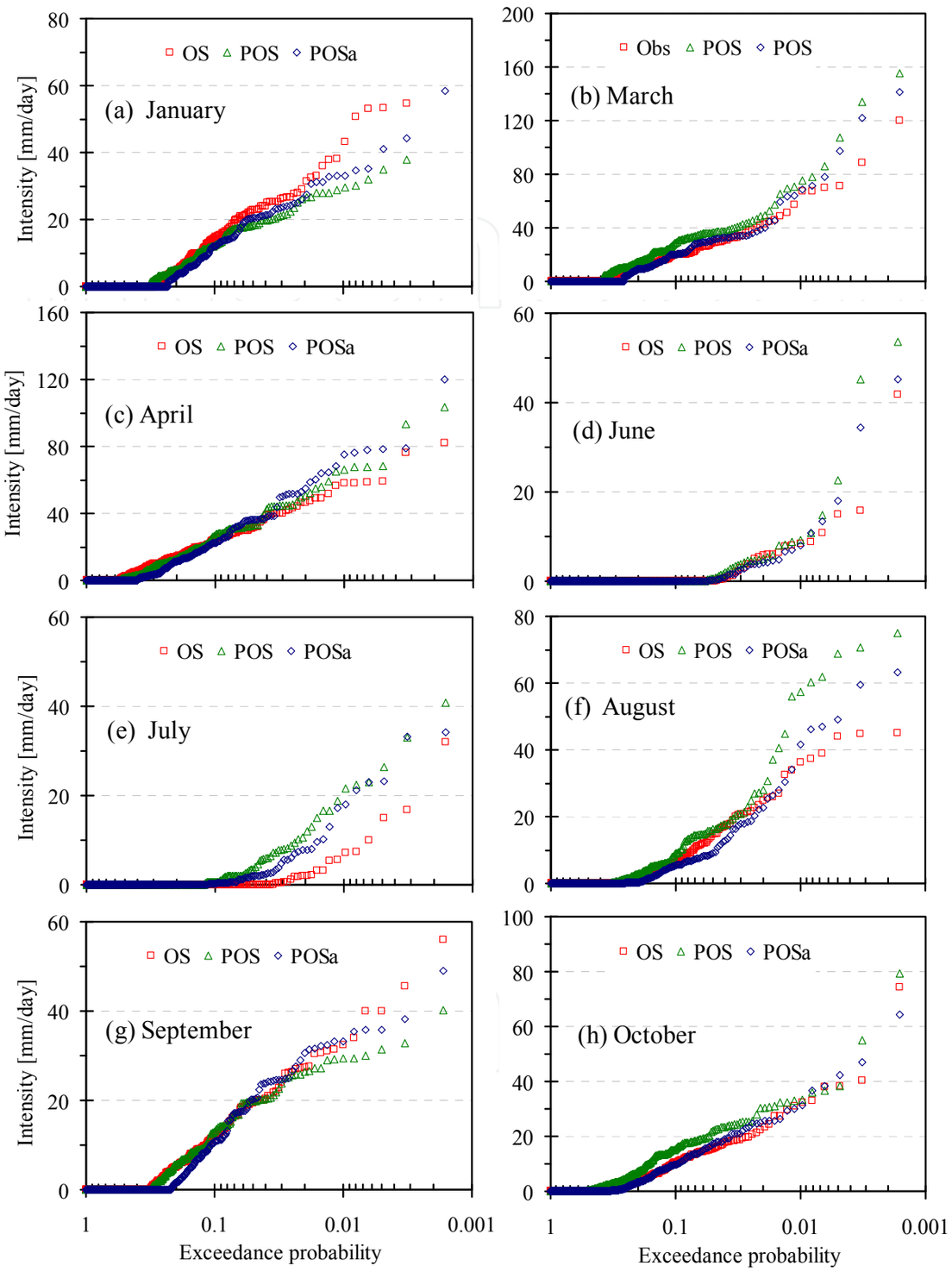

Fig. 6.12. Typical distribution of daily rainfall for an example dataset for different months for an example GCM run (CGCM3.1(T47), R2). The results are for the data extracted from a GCM grid over the Ruizi catchment. The OS is the areal rainfall over the River Ruizi catchment.

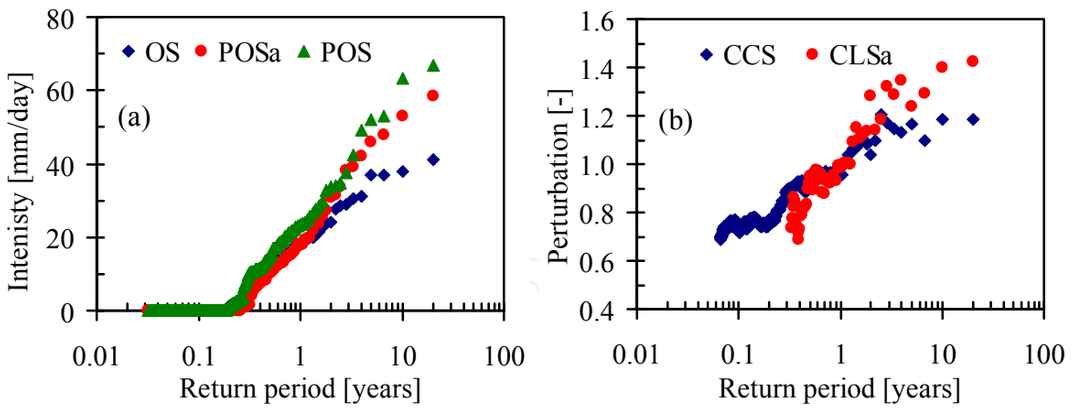

Fig. 6.13. Classical distribution for January daily rainfall (a), and the perturbations (b) derived from SS and CS (CCS) and from OS and POSa (CLSa) for a grid over the River Ruizi catchment.

9. Conclusion on downscaling

A nonparametric statistical downscaling of daily rainfall time series from GCM runs that uses a perturbation approach is formulated and demonstrated. The core of the principle lies in the verity that climate change signals can be extracted from the GCM runs (control and scenarios) in an empirical way without explicit assumption of the underlying probability distribution and applied to the observed series. The modified observed time series are the downscaled GCM results, which are plausible for climate change impacts assessment at local scale. Among the important features of the rainfall time series are wet spells, wet-day intensities, wet-day frequencies and coefficients of variation and are considered in the perturbation approach. If only wet-day intensity and wet-day frequency perturbations are considered, the resulting time series can still have similar signals of coefficient of variation. However, it leads to an overestimate of the change in wet spells and intensity. Thus, the changes in the structure of both the dry/wet spells, which are very important temporal features of rainfall, are not captured in the perturbed series. Since hydrological models are very sensitive to rainfall, overestimates of the change in the wet spells and rainfall intensity events may significantly influence hydrological extremes. In order to eschew and buffer these problems, consideration of the changes in the wet spells is crucial. One other advantage of the wet-spell approach for statistical downscaling using quantile perturbation approach is that the changes in the distributions of both the wet and dry spells can be validated through a graphical approach. In addition, the wet-spell approach preserves the changes in extremes of rainfall as projected by the climate models. Thus, hydrological impacts of climate change on extremes can appropriately be estimated given the fact that rainfall time series is an important input into the hydrological model.

Example of studies that have focused on the impacts of climate change on extremes include that of Taye et al. (2011), Nyeko-Ogiramoi et al. (2011), Willems and Vrac (2011), and Willems et al. (2011 in press). A conclusive statement in Nyeko-Ogiramoi (2011) states that for the Lake Victoria basin, the impact of climate change on the intensity and frequency of precipitation extremes and daily maximum temperature are projected to be significant in the 2050s and 2090s. It further states that water professionals should take into account the

expected impact of climate change on the precipitation extremes as it will significantly affect the design statistics, which is very important for many engineering applications. The importance of the assessment of the possible impacts of climate change on precipitations extremes and the implications for hydraulic engineering practices can indeed not be underlooked.

10. Acknowledgements

This research was supported by the Flemish Interuniversity Council (VLIR) and is linked to the FRIEND/Nile project of UNESCO and the Flanders in Trust Fund of the Flemish Government of Belgium. We also acknowledge this support which has initiated collaboration between Departments of Civil Engineering, Katholieke Universiteit Leuven, Belgium and Makerere University Kampala, Uganda. Thanks to Ministry of Water and Environment, Uganda for availing some of the data which facilitated the works.

11. References

Anyah, R.O. & Semazzib, F.H.M. (2007), Variability of East African rainfall based on multiyear RegCM3 simulations, *Int. Jol. Climatol.*, Vol.27, (September 2006), pp. 357–371, DOI: 10.1002/joc.1401.

Arai, T. & Kragic, D. (1999). Variability of Wind and Wind Power, In: *Wind Power,* S.M. Muyeen, (Ed.), 289-321, Scyio, ISBN 978-953-7619-81-7, Vukovar, Croatia.

Barnett, D. N., Simon, J., Murphy, B.J.M., Sexton, D.M.H., & Webb, M.J. (2006). Quantifying uncertainty in changes in extreme event frequency in response to doubled CO2 using a large ensemble of GCM simulations, *Clim. Dyn.*, Vol.26, (January 2006), pp. 489–511.

Benestad, R.E., Hanssen-Bauer, I. & Chen, D. (2008). Empirical-statistical downscaling, *World Scientific, Singapore*, ISBN: 978-981-281-912-3.

Christensen, J.H, Carter T.R. & Rummukainen, M. (2007). Evaluating the performance and utility of regional climate models: the PRUDENCE Project, *Clim Change 2007*, Vol.81, Issue S1, pp. 1-6, ISSN: 01650009, DOI: 10.1007/s10584-006-9211-6.

Christensen, J.H., Boberg, F., Christensen, O.B. & Lucas-Picher P. (2008). On the need for bias correction of regional climate change projections of temperature and precipitation, *Geophys. Res. Lett* Vol.35, L20709, (October 2008), 6pp. doi:10.1029/2008GL035694.

Diaz-Nieto, J. & Wilby, R.L. (2005). A comparison of statistical downscaling and climate change factor methods: impacts on lowflows in the river Thames, united kingdom, *Climatic Change,*Vol.69, No.2-3, pp. 245–268, DOI: 10.1007/s10584-005-1157-6.

Fowler, H.J., Blenkinsopa, S. & Tebaldib, C. (2007). Review: Linking climate change modelling to impacts studies: recent advances in downscaling techniques for hydrological modelling. *Int. J. Climatol*. Vol.27, (September 2007), 1547–1578, DOI: 10.1002/joc.1556.

Harrold, T.I. & Jones, R.N. (2003). Downscaling GCM rainfall: a refinement of the perturbation method, In *International Congress on Modelling and Simulation,* pp. 14–17, MODSIM2003, Townsville, Australia, 4-17 July, 2003.

Ines, A.V.M. & Hansen, J.W. (2006). Bias correction of daily GCM rainfall for crop simulation studies, *Agric For Meteorol,* Vol.138, (March 2006), pp. 138:44–53, doi:10.1016/j.agrformet.2006.03.009.

IPCC (2001a). Climate change: the scientific basis, pp. 996, Cambridge University Press, Cambridge and New York, NY, USA, available online.

Kharin, V.V. & Zwiers, F.W. (2005). Estimating extremes in transient climate change simulations, *J. Clim.*, Vol.18, (September 2004), pp. 1156–1173.

Lall, U. (1995). Nonparametric function estimation: Recent hydrologic applications. *Reviews of Geophysics*, Vol.33, Iss.S1, pp. 1093–1102, doi: 10.1029/95RG00343.

Lall, U., Rajagopalan, B. & Tarboton, D.G. (1996). A nonparametric wet/dry spell model for resampling daily Precipitation. *Water Resour. Res*. Vol.32, No.9, (September 1996), pp. 2803–2823.

Lenderink, G., Buishand, A. & van Deursen, W. (2007). Estimates of future discharges of the river Rhine using two scenario methodologies: direct versus delta approach, *Hydrol. Earth Syst. Sci*., 11, 1145–1159.

Li, B.; Xu, Y. & Choi, J. (1996). Applying Machine Learning Techniques, *Proceedings of ASME 2010 4th International Conference on Energy Sustainability*, pp. 14-17, ISBN 842-6508-23-3, Phoenix, Arizona, USA, May 17-22, 2010

Lima, P.; Bonarini, A. & Mataric, M. (2004). *Application of Machine Learning,* InTech, ISBN 978-953-7619-34-3, Vienna, Austria

MathWorks Inc, MATLAB (2008). Application programme interface reference version 7.0. *The MathWorks Inc*., Natick, MA, USA, pp. 01760-2098.

Meehl, G.A., Stocker, T.F., Collins, W.D., Friedlingstein, P., Gaye, A.T., Gregory, J.M., Kitoh, A., Knutti, R., Murphy, J. M., Noda, A., Raper, S. C. B., Watterson, I. G., Weaver A.J., & Zhao, Z.-C. (2007). Global Climate Projections. In: Climate Change 2007: The Physical Science Basis. Contribution of Working Group I to the Fourth Assessment Report of the Intergovernmental Panel on Climate Change [Solomon, S., D. Qin, M. Manning, Z. Chen, M. Marquis, K.B. Averyt, M. Tignor and H.L. Miller (eds.)]. *Cambridge University Press, Cambridge*, United Kingdom and New York, NY, USA, pp. 747-846.

Nakicenovic, N., Alcamo, J., Davis, G., de Vries, B., Fenhann, J., Gaffin, S., Gregory, K., Grübler, A., Jung, T. Y., Kram, T., La Rovere, E. L., Michaelis, L., Mori, S., Morita, T., Pepper, W., Pitcher, H., Price, L., Riahi, K., Roehrl, A., Rogner, H.-H., Sankovski, A., Schlesinger, M., Shukla, P., Smith, S., Swart, R., van Rooijen, S., Victor, N. & Dadi Z. (2000). IPCC Special Report on Emissions Scenarios. Cambridge University Press, Cambridge, United Kingdom and New York, NY, USA. 599pp.

Ntegeka, V., (2011). Assessment of the observed and future climate variability and change in hydroclimatic and hydrological extremes. *PhD dissertation*, Arenberg Doctoral school of Science, Engineering and Technology, Katholieke Universiteit Leuven, Belgium.

Nyeko-Ogiramoi, P, Willems, P. & Ngirane-Katashaya, G. (2011). Assessment of the impact of climate change on extreme precipitation and temperature events over the upper River Nile basin, *Proceeding of the Advances in Engineering & Technology international conference, 1410AET2011*-(109), January 30 – February 1, 2011, Entebbe, Uganda.

Nyeko-Ogiramoi, P., Ngirane-Katashaya, G., Willems, P. & Ntegeka, V. (2010). Evaluation and inter-comparison of Global Climate Models' performance over Katonga and Ruizi catchments in Lake Victoria basin, *Phy. Chem. Earth*, Vol.35, Iss.13-14, (August 2010), pp. 618–633, doi: 10.1016/j.pce.2010.07.037.

Olsson, J., Berggren, K., Olofsson, M., & Viklander, M. (2009). Applying climate model precipitation scenarios for urban hydrological assessment: A case study in Kalmar City, Sweden. *Atmos. Res*., Vol.92, (May 2009), Iss. 3, pp. 364–375, doi: doi:10.1016/j.atmosres.2009.01.015

Piani, C., Haerter, J. O. & Coppola, E. (2010). Statistical bias correction for daily precipitation in regional climate models over Europe, *Theor Appl Climatol*., Vol.99, No.1-2, (April 2009), pp. 187–192, doi: 10.1007/s00704-009-0134-9.

Prudhomme, C., Reynard, N. & Crooks, S (2002). Downscaling of global climate models for flood frequency analysis: Where are we now?, *Hydrol. Process*., Vol.16, No. (March 2002), pp.1137–1150.

Rajagopalan, B. & Lall, U., 1999. A *k*-nearest-neighbor simulator for daily precipitation and other variables, *Water Resour. Resear*. Vol.35, No.10, (October 1999), 3089–3101.

Rajagopalan, B., Lall, U., Tarboton, D. G. & Bowles, D. S. (1997). Multivariate nonparametric resampling scheme for generation of daily weather variables, *Stochastic Hydrol. Hydraul*. Vol.11, Iss.1, (1997) pp. 65-93.

Schmidli J. & Frei, C. (2005). Trends of heavy precipitation and wet and dry spells in Switzerland during the 20th century. *Int. J. Climatol.* Vol.25, Iss.6, (May 205), pp. 753–771, DOI: 10.1002/joc.1179.

Schulzweida, U., & Kornblueh, L. (2011). Climate Data Operators, Ver.1.5., pp. 1-164, *MPI for Meteorology*, Germany.

Siegwart, R. (2001). Indirect Manipulation of a Sphere on a Flat Disk Using Force Information. *International Journal of Advanced Robotic Systems,* Vol.6, No.4, (December 2009), pp. 12-16, ISSN 1729-8806.

Svensson, C. & Jones, D.A. (2010). Review of methods for deriving areal reduction factors, *J. Flood Risk Management* Vol.3, Iss.3,(June, 2010), pp. 232–245.

Taye, M. T., Ntegeka, V., Nyeko-Ogiramoi, N. P. & Willems, P. (2011). Assessment of climate change impact on hydrological extremes in two source regions of the Nile River Basin, *Hydrol. Earth Syst*. Sci., Vol. 15, No.1 (Januanry 2011), pp. 209-222.

Trenberth, K. E, Dai, A., Rasmussen, R. M. & Parsons, D. B. (2003), The changing character of precipitation. *Bull Am Meteorol Soc* Vol.84, (March 2003), pp. 1205–1217, doi: 10.1175/BAMS-84-9-1205.

Van der Linden, S. (June 2010). Integrating Wind Turbine Generators (WTG's) with Energy Storage, In: *Wind Power,* 17.06.2010, Available from

Willems, P. & Vrac, M. (2011). Statistical precipitation downscaling for small-scale hydrological impact investigations of climate change. *J. Hydrol.* Vol.402, (April 2011), pp.193–205.

Willems, P., Arnbjerg-Nielsen, K., Olsson, J., Nguyen, V.T.V. (2011). Climate change impact assessment on urban rainfall extremes and urban drainage: methods and shortcomings. *Atmospheric Research,*Vol.103(January 2012), pp.106-118.

Yue-Cong W. & Barry A. (2010). Climate change and its impacts on water supply and demand in Sydney, *Summary report*: NSW office for water, Sydney, NSW, pp. 12.

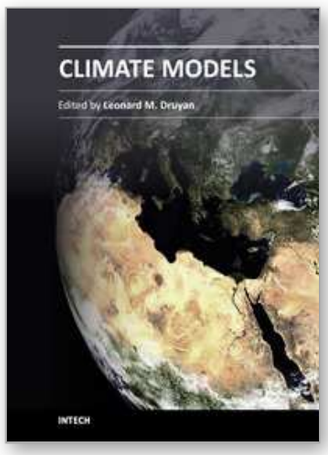

Climate Models

Edited by Dr. Leonard Druyan

ISBN 978-953-51-0135-2
Hard cover, 336 pages
Publisher InTech
Published online 02, March, 2012
Published in print edition March, 2012

Climate Models offers a sampling of cutting edge research contributed by an international roster of scientists. The studies strive to improve our understanding of the physical environment for life on this planet. Each of the 14 essays presents a description of recent advances in methodologies for computer-based simulation of environmental variability. Subjects range from planetary-scale phenomena to regional ecology, from impacts of air pollution to the factors influencing floods and heat waves. The discerning reader will be rewarded with new insights concerning modern techniques for the investigation of the natural world.

How to reference

In order to correctly reference this scholarly work, feel free to copy and paste the following:

Paul Nyeko-Ogiramoi, Patrick Willems, Gaddi Ngirane-Katashaya and Victor Ntegeka (2012). Nonparametric Statistical Downscaling of Precipitation from Global Climate Models, Climate Models, Dr. Leonard Druyan (Ed.), ISBN: 978-953-51-0135-2, InTech, Available from: http://www.intechopen.com/books/climate-models/using-global-climate-models-to-assess-the-impacts-of-climate-change-on-precipitation-extremes-at-cat

INTECH
open science | open minds

InTech Europe
University Campus STeP Ri
Slavka Krautzeka 83/A
51000 Rijeka, Croatia
Phone: +385 (51) 770 447
Fax: +385 (51) 686 166
www.intechopen.com

InTech China
Unit 405, Office Block, Hotel Equatorial Shanghai
No.65, Yan An Road (West), Shanghai, 200040, China
中国上海市延安西路65号上海国际贵都大饭店办公楼405单元
Phone: +86-21-62489820
Fax: +86-21-62489821

IntechOpen